Models of the Cytochromes. Redox Properties and Thermodynamic Stabilities of Complexes of "Hindered" Iron(III) and Iron(II) Tetraphenylporphyrinates with Substituted Pyridines and...

ARTICLE *in* INORGANIC CHEMISTRY · AUGUST 1996

Impact Factor: 4.76 · DOI: 10.1021/ic960491h

Models of the Cytochromes. Redox Properties and Thermodynamic Stabilities of Complexes of "Hindered" Iron(III) and Iron(II) Tetraphenylporphyrinates with Substituted Pyridines and Imidazoles

Marlys J. M. Nesset,* Nikolai V. Shokhirev, Paul D. Enemark, Simone E. Jacobson, and F. Ann Walker*

Department of Chemistry, University of Arizona, Tucson, Arizona 85721

Received May 8, 1996[⊗]

The Fe^{III}/Fe^{II} and Fe^{II}/Fe^{I} reduction potentials of a series of model hemes have been measured by cyclic voltammetry in dimethylformamide at 25 °C as a function of the concentration of added axial ligands. The six porphyrinate ligands utilized were tetraphenylporphyrin (TPP), tetramesitylporphyrin (TMP), and a series of "hindered" tetraphenylporphyrins having substituents (OCH_3, F, Cl, Br) on both *ortho* positions of each of the four phenyl rings. The perchlorato salts of the iron(III) porphyrinates were utilized for the titrations. The axial ligands utilized were *N*-methylimidazole, 2-methylimidazole, and pyridines of basicities ranging in $pK_a(PyH^+)$ from 9.7 to 1.1. From the electrochemical titration, the equilibrium constants (log β_2 and some log β_1) of each iron porphyrinate with each ligand were determined. The values of log β_2 for the iron(III) complexes decrease in the order Br > Cl > CH_3 > OCH_3 > H > F, while those for iron(II) decrease in the slightly modified order Br > Cl > CH_3 > F > OCH_3 > H. Rather than electronegativity or electron-donating/withdrawing characteristics, these results appear to follow primarily the physical size of the *ortho* substituents: The iron porphyrinates with the largest *ortho* substituents have the largest equilibrium constants. The hindered (TPP)Fe^{II} complexes are usually, but not always, more stable than the corresponding hindered (TPP)Fe^{III} complexes. For both (TPP)Fe^{III} and the hindered (TPP)Fe^{III} complexes, the slope of the correlation of log β_2^{III} with the pK_a of the conjugate acid of the pyridine ligand is 1.0. The equilibrium constants for hindered (TPP)Fe^{II} complexes, however, have virtually no dependence upon the base strength of the axial pyridines, while those for (TPP)Fe^{II} has a slight sensitivity, with a slope of 0.15. In contrast to common belief, 2-methylimidazole readily forms bis complexes with some iron(II) tetraphenylporphyrinates ((TMP)Fe^{II}, ((2,6-Cl_2)TPP)Fe^{II}, and ((2,6-Br_2)$_4$(TPP)Fe^{II}), although it does not with (TPP)-Fe^{II} and its (2,6-F_2)$_4$- and (2,6-(OCH_3)$_2$)$_4$- counterparts. *N*-Methylimidazole is unique among the axial ligands of this study, in that the equilibrium constants for binding to both Fe(III) and Fe(II) are virtually identical for all porphyrinates studied.

Introduction

The relationship of protein structure to the reduction potentials of the cytochromes involved in electron transfer, as well as other structure−function relationships of heme proteins, has long been of interest to many scientists. In the past, a large number of investigations of the reactions and physical and chemical properties of synthetic metalloporphyrins have been carried out to probe the electronic factors involved in the hope of providing further insight into the reactivity and spectroscopic properties of the heme proteins.[1−15] In most of these studies, symmetrically tetra-*para*- or tetra-*meta*-substituted tetraphenylporphyrins and their metal complexes were used, and important information was gained concerning the sensitivity of the properties of interest (formation constants for axial ligand complexes, reduction potentials, NMR chemical shifts, EPR *g* values, electronic and vibrational spectra, etc.) to the electronic properties of the substituents, X. However, among these many investigations, little or no attention has been given to the effects of phenyl *ortho* substituents on these properties, except for EPR, Mössbauer, and molecular structural investigations of the bis-(imidazole),[16] -(substituted pyridine),[17] and -(1,2-dimethylimidazole)[18] complexes of (tetramistylporphyrinato)iron(III) per-

[⊗] Abstract published in *Advance ACS Abstracts,* August 1, 1996.

(1) Falk, J. E. *Porphyrins and Metalloporphyrins*; Elsevier: New York, 1964; pp 28, 42, 69, 93.
(2) Balke, V. L.; Walker, F. A.; West, J. T. *J. Am. Chem. Soc.* **1985**, *107*, 1226 and references therein.
(3) (a) Walker, F. A.; Hui, E.; Walker, J. M. *J. Am. Chem. Soc.* **1975**, *97*, 2390. (b) Walker, F. A. *J. Am. Chem. Soc.* **1973**, *95*, 1150. (c) Walker, F. A. *J. Am. Chem. Soc.* **1973**, *95*, 1154. (d) Walker, F. A.; Beroiz, D.; Kadish, K. M. *J. Am. Chem. Soc.* **1976**, *98*, 3484.
(4) Walker, F. A.; Lo, M. W.; Ree, M. T. *J. Am. Chem. Soc.* **1976**, *98*, 5552.
(5) (a) Satterlee, J. D.; La Mar, G. N.; Frye, J. S. *J. Am. Chem. Soc.* **1976**, *98*, 9295. (b) Satterlee, J. D.; La Mar, G. N.; Bold, T. J. *J. Am. Chem. Soc.* **1977**, *99*, 1088.
(6) Vogel, G. C.; Beckman, B. A. *Inorg. Chem.* **1976**, *15*, 483.
(7) McDermott, G. A.; Walker, F. A. *Inorg. Chim. Acta* **1984**, *91*, 95.
(8) Walker, F. A.; Barry, J. A.; Balke, V. L.; McDermott, G. A.; Wu, M. Z.; Linde, P. F. *Adv. Chem. Ser.* **1982**, *201*, 377.
(9) Kadish, K. M.; Morrison, M. M.; Constant, L. A.; Dickens, L.; Davis, D. G. *J. Am. Chem. Soc.* **1976**, *98*, 8387.
(10) Kadish, K. M.; Bottomley, L. A. *J. Am. Chem. Soc.* **1977**, *99*, 2380.
(11) Walker, F. A.; Simonis, U. Proton NMR Spectroscopy of Model Hemes. In *Biological Magnetic Resonance: NMR of Paramagnetic Molecules*; Berliner, L. J., Reuben, J., Eds.; Plenum Press: New York, 1993; Vol. 12, pp 133−274.
(12) Toney, G. E.; Gold, A.; Savrin, J.; ter Haar, L. W.; Sangaiah, R.; Hatfield, W. E. *Inorg. Chem.* **1984**, *23*, 4350.
(13) (a) Walker, F. A. *J. Am. Chem. Soc.* **1970**, *92*, 4235. (b) Walker, F. A.; Reis, D.; Balke, V. L. *J. Am. Chem. Soc.* **1984**, *106*, 6888.
(14) Hagen, K. I.; Schwab, C. M.; Edwards, J. O.; Jones, J. G.; Lawler, R. G.; Sweigert, D. A. *J. Am. Chem. Soc.* **1988**, *110*, 7024.
(15) (a) Mink, L. M.; Christensen, K. A.; Walker, F. A. *J. Am. Chem. Soc.* **1992**, *114*, 6930. (b) Mink, L M.; Polam, J. R.; Christensen, K. A.; Bruck, M. A.; Walker, F. A. *J. Am. Chem. Soc.* **1995**, *117*, 9329.
(16) Safo, M. K.; Gupta, G. P.; Walker, F. A.; Scheidt, W. R. *J. Am. Chem. Soc.* **1991**, *113*, 5497.
(17) Safo, M. K.; Gupta, G. P.; Watson, C. T.; Simonis, U.; Walker, F. A.; Scheidt, W. R. *J. Am. Chem. Soc.* **1992**, *114*, 7066.
(18) Munro, O. Q.; Marques, H. M.; Debrunner, P. G.; Mohanrao, K.; Scheidt, W. R. *J. Am. Chem. Soc.* **1995**, *117*, 935.

S0020-1669(96)00491-0 CCC: $12.00

chlorate. In order to understand the chemical reactivity of (TMP)Fe and other related complexes, we have used the "hindered" iron tetraphenylporphyrinates ("hindered" = phenyl rings substituted at positions 2 and 6), which have previously been used to model cytochrome P450,[19−26] to obtain a better understanding of the factors that affect the redox and ligand-binding behavior of the bis(histidine)-coordinated cytochromes. The use of a number of hindered iron tetraphenylporphyrinates allows modeling of both electronic and structural effects of phenyl substituents on the reduction potential and the ability of the iron to form complexes with axial ligands such as imidazoles and pyridines, while maintaining a relatively constant amount of "protection" of the porphyrinate ring from solvation.

For other iron(III) porphyrinates, the complexing ability, as measured by the equilibrium constants, has been shown to depend upon the anion associated with the iron(III) center, the solvent, and the steric and electronic properties (basicity) of the axial ligands and the porphyrinate.[4] The results of a large number of measurements of the equilibrium constants for axial ligation to iron(III) and iron(II) tetraphenylporphyrinates as a function of solvent and anion have been summarized elsewhere.[27] The variety of conditions and methods utilized for measuring these equilibrium constants and the dearth of information concerning the effects of phenyl *ortho* substituents on the stability of the complexes with a well-chosen series of axial ligands, as well as a desire to model the redox behavior of the bis(histidine)-coordinated cytochromes, are the reasons that we have carried out this study.

There are three commonly used methods for measuring the equilibrium constants for axial ligation of model heme compounds: UV−visible spectroscopy,[2,4,28−31] NMR spectroscopy,[32] and electrochemical techniques.[8,9,33−37] (See ref 34 for a review of the last subject.) Electrochemical methods are preferred from an experimental point of view because, in one set of experiments, both the iron(III) and the iron(II) equilibrium constants can be evaluated. In the NMR method, the equilibrium constants are usually measured by integrating the proton resonances of the bound and unbound metal porphyrinate species and the free ligand. The integrations are not accurate when the metal porphyrinate complex is in fast or intermediate exchange with the ligand-free metal porphyrinate and free-ligand starting materials, and thus NMR measurements often require temperatures far below room temperature where ligand exchange is slow on the NMR time scale. However, since the enthalpies of ligand addition (and in this study, ligand replacement) are negative, formation constants become larger as the temperature is lowered. Thus the equilibrium constants measured by NMR may be too large to measure at the concentrations required for NMR spectroscopy.

UV−visible techniques have the advantage of being applicable to very dilute solutions, where it is possible to measure much larger equilibrium constants. However, for both NMR and UV−visible techniques, the constants for axial ligand complexation of only one oxidation state can be measured at one time, and the air sensitivity of Fe(II) porphyrinates complicates measurements for this oxidation state. Thus, electrochemical techniques based upon cyclic voltammetry are preferred when air-sensitive species are involved, as well as for the expediency of measuring both Fe(III) and Fe(II) binding constants at the same time. Furthermore, not only the binding constants of ligands to at least two oxidation states of a metal but also the reduction potential for the couple, in the absence and presence of axial ligand, can be evaluated from the same data set.

In this study, the equilibrium constants for complex formation of several "hindered" iron porphyrinates with various pyridines or imidazoles have been determined by utilizing cyclic voltammetry. When the equilibrium constant for the addition of the second pyridine or imidazole (K_2) is not large, the stepwise equilibrium constants can be determined. Reactions illustrating the binding of one or two axial ligands to Fe(II) and Fe(III) porphyrinates are given by eqs 1−4. We have included the DMF molecules known or believed to be coordinated to each oxidation state of each complex, as will be discussed further below. For most iron porphyrinates, however, K_2 is larger than

$$[(TPP)Fe(DMF)] + L \rightleftharpoons [(TPP)Fe(L)] + DMF \quad K_1^{II} \quad (1)$$

$$[(TPP)Fe(L)] + L \rightleftharpoons [(TPP)Fe(L)_2] \quad K_2^{II} \quad (2)$$

$$[(TPP)Fe(DMF)_2]^+ClO_4^- + L \rightleftharpoons [(TPP)Fe(L)(DMF)] + ClO_4^- + DMF \quad K_1^{III} \quad (3)$$

$$[(TPP)Fe(L)(DMF)]^+ClO_4^- + L \rightleftharpoons [(TPP)Fe(L)_2]^+ClO_4^- + DMF \quad K_2^{III} \quad (4)$$

K_1 for both oxidation states, and hence usually only the overall

(19) (a) Groves, J. T.; Haushalter, R. C.; Nakamura, M; Nemo, T.; Evans, B. J. *J. Am. Chem. Soc.* **1981**, *103*, 2884. (b) Groves, J. T.; Nemo, T. E. *J. Am. Chem. Soc.* **1983**, *105*, 6243. (c) Groves, J. T.; Watanabe, Y. *J. Am. Chem. Soc.* **1986**, *108*, 507, 7884.

(20) (a) Traylor, T. G.; Tsuchiya, S. *Inorg. Chem.* **1987**, *26*, 1338. (b) Traylor, T. G.; Tsuchiya, S. *Inorg. Chem.* **1988**, *27*, 4520. (c) Traylor, T. G.; Xu, F. *J. Am. Chem. Soc.* **1988**, *110*, 1953. (d) Traylor, T. G.; Nakano, T.; Miksztal, A. R.; Dunlap, B. E. *J. Am. Chem. Soc.* **1987**, *108*, 7861. (e) Traylor, T. G.; Hill, K. W.; Fann, W.-P.; Tsuchiya, S.; Dunlap, B. E. *J. Am. Chem. Soc.* **1992**, *114*, 1308. (f) Traylor, T. G.; Tsuchiya, S.; Byun, Y.-S.; Kim, C. *J. Am. Chem. Soc.* **1993**, *115*, 2775.

(21) (a) Gold, A.; Jayaraj, K.; Doppelt, P.; Weiss, R.; Chottard, G.; Bill, E.; Ding, X.; Trautwein, A. X. *J. Am. Chem. Soc.* **1988**, *110*, 5756. (b) Mandon, D.; Weiss, R.; Franke, M.; Bill, E.; Trautwein, A. X. *Angew. Chem., Int. Ed. Engl.* **1989**, *28*, 1989. (c) Mandon, D.; Weiss, R.; Jayaraj, K.; Gold, A; Terner, J.; Bill, E.; Trautwein, A. X. *Inorg. Chem.* **1992**, *31*, 4404.

(22) Maldotti, A.; Bartocci, C.; Amadelli, R.; Polo, E.; Battioni, P.; Mansuy, D. *J. Chem. Soc., Chem. Commun.* **1991**, 1487.

(23) (a) Collman, J. P.; Hampton, P. D.; Brauman, J. I. *J. Am. Chem. Soc.* **1990**, *112*, 2977 and 2986. (b) Collman, J. P.; Zhang, X.; Lee, V. J.; Uffelman, E. S.; Brauman, J. I. *Science* **1993**, *261*, 1404.

(24) Sugimoto, H.; Tung, H.-C.; Sawyer, D. T. *J. Am. Chem. Soc.* **1988**, *110*, 2465.

(25) Watanabe, Y.; Ishimura, Y. *J. Am. Chem. Soc.* **1989**, *111*, 410.

(26) Ostović, D.; Bruice, T. C. *Acc. Chem. Res.* **1992**, *25*, 314 and references therein.

(27) Walker, F. A.; Simonis, U. Iron Porphyrin Chemistry. In *Encyclopedia of Inorganic Chemistry*; King, R. B., Ed.; Wiley & Sons: Chichester, U.K., 1994; Vol. 4, pp 1785−1846.

(28) Hashimoto, T.; Dyer, R. L.; Crossley, M. J.; Baldwin, J. E.; Basolo, F. *J. Am. Chem. Soc.* **1982**, *104*, 2101.

(29) Brewer, C. T.; Brewer, G. A. *Inorg. Chem.* **1987**, *26*, 3420.

(30) Portela, C. F.; Magde, D.; Traylor, T. G. *Inorg. Chem.* **1993**, *32*, 1313.

(31) Koerner, R.; Wright, J. L.; Nesset, M. J. M.; Ding, D.; Aubrecht, K.; Watson, R. A.; Barber, R. A.; Mink, L. M.; Tipton, A. R.; Norvell, C. J.; Simonis, U.; Walker, F. A. To be submitted.

(32) (a) Nakamura, M. *Inorg. Chim. Acta* **1989**, *161*, 73. (b) Nakamura, M.; Nakamura, N. *Chem. Lett.* **1990**, 181. (c) Nakamura, M.; Tajima, K.; Tada, K.; Ishizu, K.; Nakamura, N. *Inorg. Chim. Acta* **1994**, *224*, 113.

(33) Bottomley, L. A.; Kadish, K. M. *Inorg. Chem.* **1980**, *19*, 832.

(34) Kadish, K. M. In *Iron Porphyrins*; Lever, A. B. P., Gray, H. B., Eds.; Addison-Wesley: Reading, MA, 1984.

(35) Lexa, D.; Momenteau, M.; Mispelter, J.; Lhoste, J. M. *Bioelect. Bioenerg.* **1974**, *1*, 108.

(36) Lexa, D.; Momenteau, M.; Mispelter, J. *Biochim. Biophys. Acta* **1974**, *338*, 151.

(37) Lexa, D.; Saveant, J. M. In *Redox Chemistry and Interfacial Behaviour of Biological Molecules*; Dryhurst, G., Niki, K., Eds.; Plenum: New York, 1988, 1993; pp 1−25.

constants for bis(ligand) complex formation can be determined according to eqs 5 and 6.[8,10,33−35,38] The complete expression

$$[(TPP)Fe(DMF)] + 2L \rightleftharpoons [(TPP)Fe(L)_2] + DMF \quad \beta_2^{II} \quad (5)$$

$$[(TPP)Fe(DMF)_2]^+ClO_4^- + 2L \rightleftharpoons [(TPP)Fe(L)_2]^+ClO_4^- + 2DMF \quad \beta_2^{III} \quad (6)$$

describing the relationship of these equilibria to the Nernst equation is shown by (7), where β_1^{III} ($=K_1^{III}$) and β_1^{II} ($=K_1^{II}$)

$$(E_{1/2})_c = (E_{1/2})_s - \frac{RT}{nF}\ln\frac{1+\beta_1^{III}[L]+\beta_2^{III}[L]^2}{1+\beta_1^{II}[L]+\beta_2^{II}[L]^2} \quad (7)$$

represent the equilibrium constants for binding one axial ligand, $(E_{1/2})_c$ is the reduction potential of the iron porphyrinate in the presence of a particular concentration of axial ligand, and $(E_{1/2})_s$ is the reduction potential of the ligand-free iron porphyrinate starting material. In cases where only one step of complex formation is observed for each oxidation state (for example, $\beta_1^{III}[L] \ll \beta_2^{III}[L]^2 \gg 1$, and the analogous situation for $\beta_1^{II}[L]$), eq 7 reduces to[39]

$$(E_{1/2})_c = (E_{1/2})_s - \frac{2.303RT}{nF}\log\frac{\beta_p^{ox}}{\beta_q^{red}} - \frac{2.303RT}{nF}\log[L]^{p-q} \quad (8)$$

where β_p^{ox} and β_q^{red} are the equilibrium constants of the oxidized species with p axial ligands and the reduced species with q axial ligands, respectively, where p and q may be 0, 1, or 2 in the case of a metalloporphyrinate.

If one oxidation state, for example, the reduced state in the Fe^{II}/Fe^{I} redox couple, does not bind axial ligands over the concentration range of interest, then eq 7 reduces to

$$(E_{1/2})_c = (E_{1/2})_s - \frac{2.303RT}{nF}(\log\beta_p^{ox}) - \frac{2.303RT}{nF}\log[L]^p \quad (9)$$

In such cases, $\log \beta_2^{II}$ can be directly determined from the concentration dependence of the Fe^{II}/Fe^{I} potential using eq 9 and then utilized in eq 8 with reduction potential data for the Fe^{III}/Fe^{II} couple, where $\log \beta_2^{III}$ is then the only unknown. However, in many cases, $\log \beta_2^{II}$ can also be calculated from the variable ligand concentration data for the Fe^{III}/Fe^{II} redox couple if a similar situation to the Fe^{II}/Fe^{I} redox couple is found, where Fe(III) does not compete for axial ligands at low concentrations. Examples of these situations will be illustrated under Results and Discussion.

The use of the simplified equations (8) and (9) is limited to situations where there is only one step of ligand addition for each oxidation state of the metal over a given ligand concentration range.[34] In cases where the equilibrium constants for each ligation step are not several orders of magnitude different from one another, there will exist a mixture of ligation states during some portion of the titration. In these cases, eqs 8 and 9 do not adequately represent the system, and the complete equation (7) must be solved using curve-fitting procedures, as described below, to correctly ascertain the equilibrium constants for both the mono- and bis-ligation states of iron(III) and iron(II).

This study reports the reduction potentials and equilibrium constants of each of five different "hindered" (tetraphenylporphyrinato)iron complexes, as well as the parent (tetraphenylporphyrinato)iron, with each of the six nitrogenous bases, 4-cyanopyridine, pyridine, 3,4-lutidine, 4-(dimethylamino)pyridine, *N*-methylimidazole, and 2-methylimidazole in dimethylformamide. DMF is itself a coordinating ligand, as emphasized in eqs 1−6, and thus the equilibrium constants we have measured are actually ligand competition constants. Utilizing the information obtained, $E_{1/2}$ and $\log \beta_2$ values, insight can be gained into the role of size and electronic effects of the phenyl 2,6 substituents on the (tetraphenylporphyrinato)iron center with regard to the stability of the complexes and their reduction potentials. The possible role of these phenyl *ortho* substituents in encouraging ruffling of the porphyrinate ring, as well as the relationship of these complexes to the cytochromes involved in electron transfer processes in biological systems, will also be considered.

Experimental Section

The (perchlorato)iron(III) forms of the following porphyrinates were used for the electrochemical experiments: tetraphenylporphryin (TPP), tetramesitylporphyrin (TMP), tetrakis(2,6-dichlorophenyl)porphyrin ($(2,6\text{-}Cl_2)_4$TPP), tetrakis(2,6-dibromophenyl)porphyrin ($(2,6\text{-}Br_2)_4$TPP), tetrakis(2,6-difluorophenyl)porphyrin ($(2,6\text{-}F_2)_4$TPP), and tetrakis(2,6-dimethoxyphenyl)porphyrin ($(2,6\text{-}(OCH_3)_2)_4$TPP). The syntheses of these compounds are described elsewhere.[40] High-purity dimethylformamide (DMF) (Burdick & Jackson) was purchased from Baxter Scientific and usually used as received. Once opened, the bottles of DMF were stored under argon in a nitrogen-filled glovebag. Purity of the DMF was easily evaluated by observing the cyclic voltammogram of the DMF containing experimental concentrations of tetrabutylammonium perchlorate (TBAP, Southwestern Chemical Co.) as electrolyte. Formic acid, one of the products of the reaction of DMF with water, is reduced at approximately −1.4 V versus Ag/Ag^+. When the formic acid reduction peak was observed, the DMF purity was not suitable for electrochemical studies and required vacuum distillation.

All pyridines and imidazoles were purchased from Aldrich. The solid compounds and liquids in Sure-Seal bottles were used as received. All other liquids were distilled prior to use. The TBAP was vacuum-dried prior to use in an ambient-temperature vacuum oven for at least 24 h and stored in a desiccator.

Cyclic voltammetric measurements were performed with a Princeton Applied Research Model 175 potentiostat equipped with a Model 276 Computer Interface Module. All electrodes were purchased from Bioanalytical Systems, Inc. The three electrodes used consisted of a platinum disk working electrode, a platinum wire counter electrode, and a silver/silver ion reference electrode (+0.452 V versus SCE). The reference electrode solvent consisted of dimethylformamide, 0.1, 0.06, or 0.03 M TBAP (to match the bulk solution in the electrochemical cell and thus minimize the junction potential), and 0.01 M $AgNO_3$. The platinum disk working electrode was cleaned before each experiment according to the polishing/rinsing procedure recommended by Bioanalytical Systems, Inc.

The solutions used for electrochemistry varied in concentration from 1 mM for the (tetraphenylporphyrinato)iron(III) perchlorate studies to 0.25 mM for all the hindered (tetraphenylporphyrinato)iron(III) perchlorates because of their low solubility. The electrolyte was used in 100-fold excess of the iron porphyrin species in each case and was 100 Mm for the $(TPP)Fe^{III}OClO_3$ experiments and 30 mM for the hindered $(TPP)Fe^{III}OClO_3$ experiments. The temperature of the water-jacketed electrochemical cell was maintained at 25.0 ± 0.2 °C for all measurements. All solutions were deoxygenated with argon for at least 10 min before each measurement. A blanket of argon was maintained over the electrochemical solution at all times. Great care had to be taken to ensure positive pressure of argon in the electrochemical cell to prevent air and moisture from entering and reacting with the DMF or the iron porphyrinate.

(38) Lexa, D.; Rentien, P.; Savéant, J. M.; Xu, F. *J. Electroanal. Chem. Interfacial Electrochem.* **1985**, *191*, 253.
(39) Kolthoff, I. M.; Lingane, J. J. *Polarography* **1952**, *1*, 221.
(40) Nesset, M. J. M.; Shokhirev, N. V.; Jacobson, S. E.; Jayaraj, K.; Gold, A.; Walker, F. A. Manuscript in preparation.

The potentiostat was controlled by a personal computer which was connected to the PAR Model 276 Computer Interface Module with an IEEE cable; communications were enabled with a GPIB board and software from National Instruments, Inc. The software controlling the potentiostat was Headstart by PAR. A program written locally converted the data taken with the Headstart program into a format recognized by the Quattro spreadsheet program.

Cyclic voltammograms were obtained at a scan rate of 50 mV/s unless otherwise stated. The scan window was 0 to −1.9 V. Current readings were taken every 4 mV, resulting in a total of 950 data points per CV scan. While the 4 mV sampling regime and a scan rate of 50 mV/s were maintained, some of the data taken were of the Fe^{III}/Fe^{II} and the Fe^{II}/Fe^{I} couples individually to ensure that neither part of either redox couple was the result of chemical reactions. No differences in either redox couple were ever observed, and therefore, the bulk of the cyclic voltammograms were obtained by observing both redox couples in the same scan. Cyclic voltammetry was performed systematically on each of the six (tetraphenylporphyrinato)iron(III) perchlorates in DMF with each of the six different axial ligands. The reduction potentials were determined from the midpoint of the anodic and cathodic peak potentials. Peak separation was calculated from the difference in the anodic and cathodic peak potentials.

Approximately 2 mg of ferrocene was added to each solution at the end of each experiment (resulting concentration ∼0.4 mM) and its $E_{1/2}$ was measured; the ferrocenium/ferrocene potential of each different iron porphyrinate solution in DMF in the absence of added axial ligand was also measured separately. The resulting potentials were +26 ± 3 mV vs Ag/Ag^+ for the solutions having 0.1 M TBAP and 33−34 ± 3 mV for the solutions having 0.03 M TBAP, a very small change over this range of electrolyte concentrations. The ferrocenium/ferrocene potential serves as an internal standard, thus ensuring that electrochemical conditions are reproducible from one measurement to the next and enabling comparisons of this work to those from other laboratories. Periodic checks of the potential at the beginning and end of the titration versus an external laboratory SCE were also made and showed that the Ag^+/Ag potential remained at a value of +452 ± 3 mV vs SCE under all experimental conditions.

Several estimates of the equilibrium constants were also obtained by visible spectrophotometry on a Hewlett-Packard 8451A photodiode array spectrophotometer. For those studies, (tetraphenylporphyrinato)-iron(III) perchlorate/ligand solutions were made immediately before use in the same brand of DMF as was used for the electrochemical studies. The measurements were carried out in a water-jacketed cell maintained at 25.0 ± 0.2 °C.

Results and Discussion

Analysis of Cyclic Voltammograms. Typical cyclic voltammograms obtained for the iron tetraphenylporphyrinates of this study are shown in Figures 1−3 for the three types of ligand concentration dependences observed. The CV waves in the absence of ligand are typical of those of other iron porphyrinates[8,9,35,36] (solid lined traces in Figures 1 and 3), with sharp anodic and cathodic peaks that indicate there is no competition for the axial positions between the solvent and the perchlorate anion. It was shown previously that DMF completely displaces the perchlorate anion from the coordination sphere of the iron-(III), resulting in high-spin six-coordinate bis-DMF complexes for Fe(III) and high-spin five-coordinate mono-DMF complexes for iron(II) porphyrinates, as shown in eqs 1−6.[11,27]

All potentials were measured versus the Ag^+/Ag reference electrode, using 0.01 M $AgNO_3$ in DMF and either 0.1 or 0.03 M TBAP electrolyte (except in the case of the single titration where the potential scan was extended to −2.2 V, shown in Figure 4), in order to match the electrolyte concentration and solvent used in the bulk solution of the (TPP)Fe and substituted (TPP)Fe samples; electrolyte concentration was maintained at ≥100 times the iron porphyrinate in all cases. The low solubility of the hindered iron tetraphenylporphyrinates precluded making 1 mM solutions for these compounds; hence their concentrations were 0.25 mM and the electrolyte concentration in these cases was 0.03 M. The lack of significant variation of the ferrocenium/ferrocene (Fc^+/Fc) potential vs the Ag^+/Ag reference electrode (+26 ± 3 mV at the beginning and +26 ± 3 mV at the end of the titrations for 0.1 M TBAP and +34 ± 3 mV at the beginning and +33 ± 3 mV at the end of the titrations for 0.03 M TBAP) and the laboratory SCE indicates that the potentials are internally self-consistent for TBAP as the electrolyte over the concentration range 0.1−0.03 M. Thus, although previous studies of the effect of cation size among tetraalkylammonium perchlorates have indicated some variation in the measured potential of an analyte with change in electrolyte *cation*,[41] we find no change in the potential of our analytes as a function of electrolyte *concentration*, at least over the range 0.03−0.10 M TBAP in DMF. Because the potentials of the Fc^+/Fc and Ag^+/Ag reference electrode were so constant vs SCE throughout the systems studied, we have listed the potentials in Table 1 vs SCE, in order that they may be more readily compared to those of other workers. The Fc^+/Fc potential of each system in the absence and presence of axial ligand is also given in Table 1.

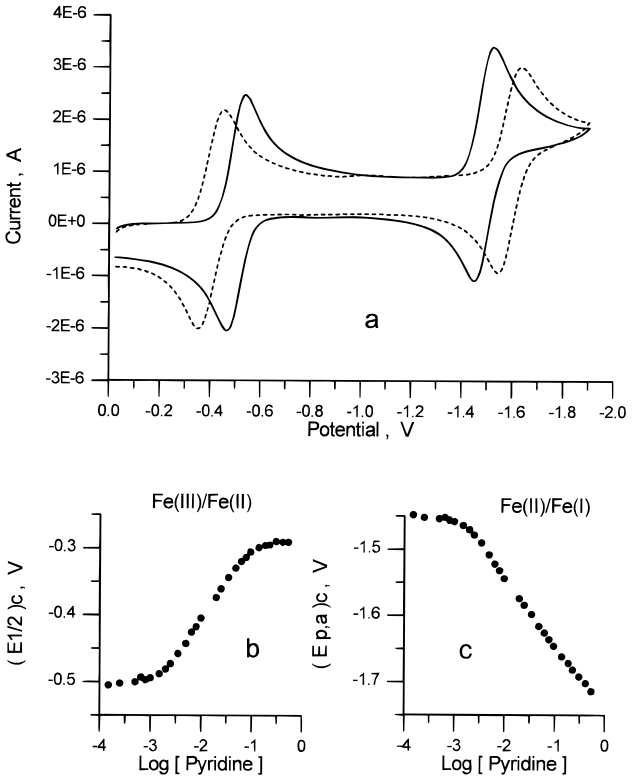

Figure 1. Example of redox couple shifts during titration and the dependence of $E_{1/2}$ on log [L] for the case $\beta_2^{II} > \beta_2^{III}$. The system shown is that of $(TPP)FeClO_4$ (1.0 mM) and pyridine in DMF (0.1 M TBAP). (a) Ligand concentrations: solid line, no pyridine; dashed line, [Py] = 1.9×10^{-2} M. All measurements were made at 25 °C with a scan rate of 50 mV/s. (b) plot of eq 8 (Fe^{III}/Fe^{II} couple) and (c) plot of eq 9 (Fe^{II}/Fe^{I} anodic peak) for the complete set of titration data.

The reduction potentials of the Fe^{III}/Fe^{II} couple of the TPP complex and the Fe^{II}/Fe^{I} couple (−0.499 and −1.492 V vs Ag^+/Ag and −0.047 and −1.040 V vs SCE, respectively) in dimethylformamide are the same as previously reported.[9,35,37,42−44] The peak separation of 70 mV for both redox couples in the absence of added ligand, although slightly larger than theoreti-

(41) Dubois, D.; Moninot, G.; Kutner, W.; Jones, M. T.; Kadish, K. M. *J. Phys. Chem.* **1992**, *96*, 7137.
(42) Bottomley, L. A.; Kadish, K. M. *Inorg. Chem.* **1981**, *20*, 1348.
(43) Kadish, K. M.; Bottomley, L. A.; Schaeper, D.; Shiue, L. R. *Bioelect. Bioenerg.* **1981**, *8*, 213.

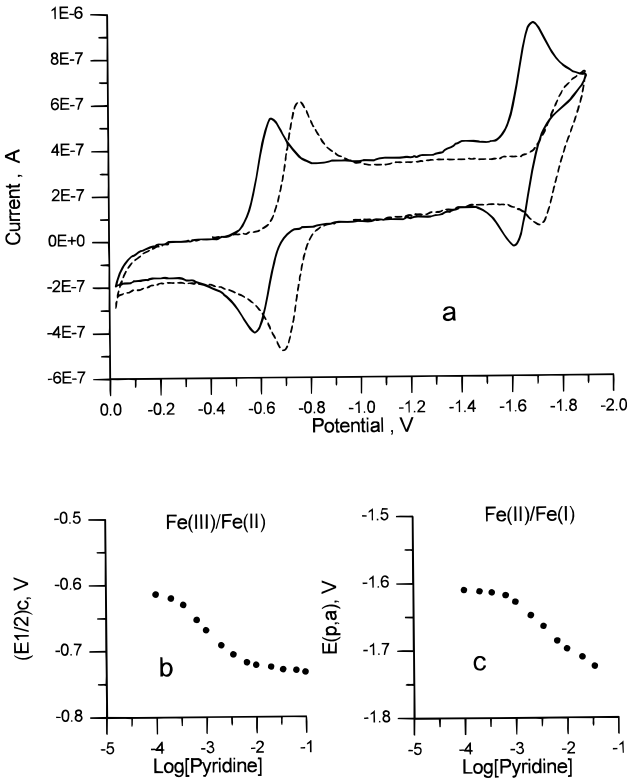

Figure 2. Example of redox couple shifts during titration and the dependence of $E_{1/2}$ on log [L] for the case $\beta_2^{III} > \beta_2^{II}$. The system shown is that of $((2,6\text{-}(OCH_3)_2)_4(TPP))FeClO_4$ (0.25 mM) and *N*-methylimidazole in DMF (0.03 M TBAP). (a) Ligand concentrations: solid line, [*N*-MeIm] = 1.0×10^{-4}; dashed line, [*N*-MeIm] = 2.0×10^{-2} M. All measurements were made at 25 °C with a scan rate of 50 mV/s. (The solid-line voltammogram shows a small peak at −1.4 V due to a small amount of formic acid, owing to decomposition of dimethylformamide in the presence of traces of water, in this sample.) (b) Plot of eq 8 (Fe^{III}/Fe^{II} couple) and (c) plot of eq 9 (Fe^{II}/Fe^{I} anodic peak) for the complete set of titration data.

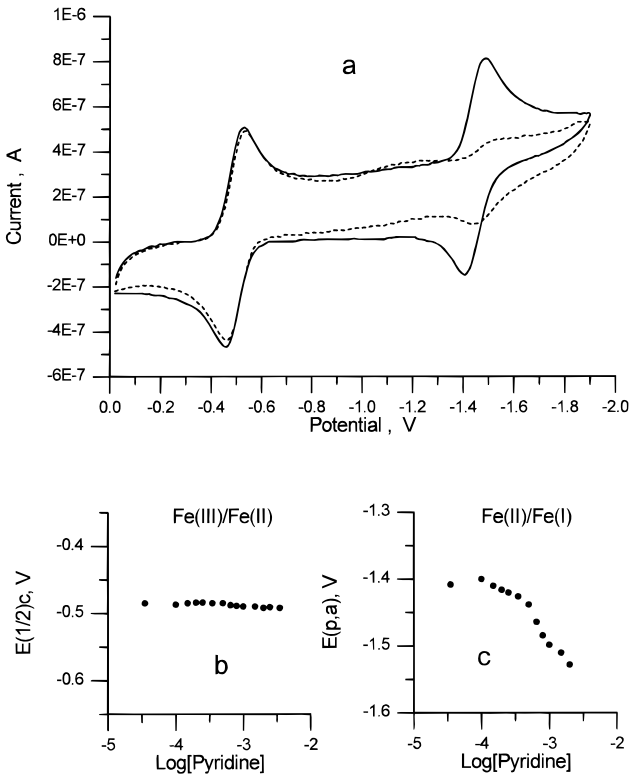

Figure 3. Example of redox couple shifts during titration and the dependence of $E_{1/2}$ on log [L] for the case $\beta_2^{III} = \beta_2^{II}$. The system shown is that of $((2,6\text{-}Br_2)_4TPP)FeClO_4$ (0.25 mM) and 4-(dimethylamino)pyridine in DMF (0.03 M TBAP). (a) Ligand concentrations: solid line, no 4-NMe_2Py; dashed line, [4-NMe_2Py] = 3.5×10^{-4} M. All measurements were made at 25 °C with a scan rate of 50 mV/s. (b) Plot of eq 8 (Fe^{III}/Fe^{II} couple) and (c) plot of eq 9 (Fe^{II}/Fe^{I} anodic peak) for the complete set of titration data.

cal,[45] is also typical for iron porphyrinates and indicates a reversible one-electron reaction. Multiple scan rate analysis reveals that $E_{p,a}$ and $E_{p,c}$ remain constant with $v^{1/2}$ (v = scan rate in volts per second), indicating reversible behavior. The anodic and cathodic reduction potentials remain constant with scan rate for the Fe^{III}/Fe^{II} redox couple when both oxidation states are biscomplexed with added ligand L, where the peak-to-peak separation is also 70 mV.

The ratio of $i_p/v^{1/2}$ remains constant with scan rate, indicating a pure electrochemical reaction and not an electrochemical chemical (EC) reaction. This ratio remains constant for the unligated and ligated Fe^{III}/Fe^{II} and Fe^{II}/Fe^{I} redox couples except where peak separation has become large, as will be discussed in detail below, and where autoreduction is presumed to occur. (We have observed that some pyridine ligands, including 4-(dimethylamino)pyridine, appear to autoreduce (TPP)FeO-ClO_3.) The multiple-scan rate experiments were performed not only on the scans from 0 to −1.9 V but also around each individual peak to confirm that the behavior of each redox couple is independent of the other.

For each of the (perchlorato)iron(III) tetraphenylporphyrinate/nitrogen base systems studied, a titration was performed by adding axial ligand, either a pyridine or an imidazole, stepwise to the iron porphyrinate solution. After each ligand addition, argon was passed through the solution for 10 min, followed by a scan of the electrochemical window that included both the Fe^{III}/Fe^{II} and the Fe^{II}/Fe^{I} waves (except for the occasional check for coupled chemical reactions where scans were taken around each wave). Ligand additions were continued until the Fe^{III}/Fe^{II} redox couple maintained a constant potential (except in the case of 4-cyanopyridine binding to most of the iron porphyrinates for which the β_2 values are very small). Usually, when the ligand concentration was reached for which the Fe^{III}/Fe^{II} couple had reached a constant potential, the Fe^{II}/Fe^{I} couple had become irreversible due to slow ligand exchange kinetics, which will be discussed in detail below.

Upon addition of axial ligands, the Fe^{III}/Fe^{II} redox couple usually shifts anodically, as shown in Figure 1. The anodic shift of the Fe^{III}/Fe^{II} wave is an indication that β_2^{III} is smaller than β_2^{II}. In cases where β_2^{III} is larger than β_2^{II}, the Fe^{III}/Fe^{II} couple shifts cathodically (Figure 2), or when β_2^{III} equals β_2^{II}, the Fe^{III}/Fe^{II} wave does not shift at all (Figure 3). In all cases, the Fe^{II}/Fe^{I} couple shifts cathodically, because the iron(I) equilibrium constant is so small that iron(I) does not take on axial ligands to any measurable extent at the temperatures and ligand concentrations used in this study. However, EPR studies of (TPP)Fe^{I} have shown it to be monoligated in the presence of pyridine at liquid nitrogen temperatures,[46] where β_1^{I} is expected to be much larger.

The shifts of the redox couples upon ligand addition are a consequence of the response of the system to changes in the concentration of the oxidized and reduced ligand-free iron

(44) Gueutin, C.; Lexa, D.; Momenteau, M.; Savéant, J.-M.; Xu, F. *Inorg. Chem.* **1986**, *25*, 4294.
(45) Bard, A. J.; Faulkner, L. R. *Electrochemical Methods. Fundamentals and Applications*; Wiley & Sons: New York, 1980; Chapter 6, p 213.
(46) Srivatsa, G. S.; Sawyer, D. T.; Boldt, N. J.; Bocian, D. F. *Inorg. Chem.* **1985**, *24*, 2123.

Table 1. Fe^{III}/Fe^{II} and Fe^{II}/Fe^{I} Potentials[a] for Iron Porphyrinates and the Fe^{III}/Fe^{II} Potentials of Their Bis-L Complexes[b,c]

$(2,6\text{-}X_2)_4$TPP substituent	potentials (V)		Fe^{III}/Fe^{II} potentials of bis-L complexes[a–c] (V)					
	Fe^{III}/Fe^{II} [a,b]	Fe^{II}/Fe^{I} [a,b]	4-CNPy	Py	3,4-Me_2Py	4-NMe_2Py	*N*-MeIm	2-MeImH
F[d]	0.033	−0.923	+0.549	+0.340	+0.305	+0.103	+0.093	
Cl[d]	−0.013	−0.978	+0.477	+0.245	+0.189	−0.011	+0.003	−0.115
Br[d]	−0.040	−0.995	+0.448	+0.214	+0.147	−0.039	−0.040	−0.131
H (TPP)[e]	−0.047	−1.040	+0.306	+0.162	+0.138	−0.045	−0.089	
CH_3 (TMP)[d]	−0.096	−1.084	+0.331	+0.140	+0.077	−0.121	−0.130	−0.212
OCH_3[d]	−0.160	−1.191	+0.222	−0.016	−0.092	−0.265	−0.280	

[a] Potentials ±3 mV vs SCE. [b] Solvent = dimethylformamide; temperature = 25.0 ± 0.2 °C; electrolyte = 0.1 or 0.03 M TBAP for (TPP)Fe and $((2,6\text{-}X_2)_4$TPP)Fe complexes, respectively. [c] Concentration of ligand was that required to cause no further shift of the Fe^{III}/Fe^{II} wave and ranged from 0.01 to 0.5 M in most cases, depending on system; see Figures 1−3 and text. [d] [TBAP] = 0.03 M; Fc^+/Fc potential = 33 ± 3 mV. [e] [TBAP] = 0.10 M; Fc^+/Fc potential = 26 ± 3 mV.

porphyrinates, as expressed by eq 8, where the reduction potential of the iron porphyrinate species throughout the titration, $(E_{1/2})_c$, is dependent upon the difference in the number of axial ligands in the two oxidation states, the ratio $\beta_p^{ox}/\beta_q^{red}$, and the free-ligand concentration [L]. When the difference in number of axial ligands, $p - q$, is not zero, the peak potentials will change as a function of the change in ligand concentration. When $p - q$ is zero, the reduction potential remains constant and its value is dependent only upon the equilibrium constant ratio.

For all of the iron porphyrinates studied, when complexed by the more basic nonhindered ligands of this study, *i.e.*, 3,4-lutidine, 4-(dimethylamino)pyridine, and *N*-methylimidazole, the behaviors are similar. The Fe^{III}/Fe^{II} couple behaves in a reversible manner throughout the titration. However, the Fe^{II}/Fe^{I} redox couple appears to exhibit electron transfer problems as the iron(II) becomes complexed, regardless of the basicity or type of coordinating axial ligand. The Fe^{II}/Fe^{I} behavior is evident in Figure 2, where it can be seen that the voltammogram in the presence of 2.0×10^{-3} M *N*-MeIm shows broadening of the iron(II) reduction peak. At higher concentrations, the cathodic peak continues to broaden and shift to more negative potential until it completely disappears. The anodic peak continues shifting as if the cathodic peak were well-behaved, but it gradually loses intensity and finally disappears as well when the [*N*-MeIm] is increased beyond 3.5×10^{-2} M. This irreversibility was noted previously by Walker *et al.*[8] in an electrochemical study of symmetrically and unsymmetrically substituted derivatives of (TPP)FeCl in DMF titrated with *N*-methylimidazole and by Lexa and co-workers[47] with various iron porphyrinates. The behavior of this redox couple is attributed to the slow kinetics of axial ligand dissociation from Fe(II),[8] especially as the size of β_2^{II} increases (since the dissociation rate constant, k_d, is proportional to $1/\beta_2^{II}$). The values of β_2^{II} for iron(II) porphyrinates are, in general, so large that the reactions appear to be nearly stoichiometric, and irreversibility begins to appear as soon as even a small amount of the iron(II) porphyrinate is bisligated. The irreversibility is most probably due to the slow on/off exchange rate of the axial ligands at the low-spin d^6 Fe(II) center. This hypothesis is supported by the behavior of the Fe^{II}/Fe^{I} wave when the electrochemical window is opened beyond −2 V, as shown in Figure 4 for $((2,6\text{-}Cl_2)_4$TPP)Fe titrated with pyridine. At low ligand concentrations, two reduction peaks are observed, one for the free iron(II) porphyrinate and one for the bisligated species, indicating slow ligand exchange for iron(II). If the ligand on/off rate were to be rapid, the second cathodic peak would not be observed and the one cathodic peak (the most anodic peak of Figure 4) would shift cathodically in a smooth manner as the ligand concentration is increased. In contrast to iron(II), iron(I) is not ligated at this temperature and ligand concentration, and in any case, ligand exchange on Fe(I) (low-spin d^7) should be quite rapid. Thus, immediately after reduction, ligands dissociate rapidly and on the return sweep, the iron(I) porphyrinate is in a nonligated state and the oxidation occurs at the "expected" potential governed by the β_2^{II} value for that ligand concentration. Even though the Fe^{II}/Fe^{I} redox couple is irreversible and therefore in-valid for the thermodynamic calculations of log β_2^{II}, the apparent log β_2^{II} values obtained from the anodic peak alone have been used as a check of the values obtained from the Fe^{III}/Fe^{II} redox couple and, if necessary, used as an approximate estimate of log β_2^{II}. For these estimates, we have assumed that the anodic peak behaves as expected for fast ligand on/off exchange for the Fe(I) oxidation state.

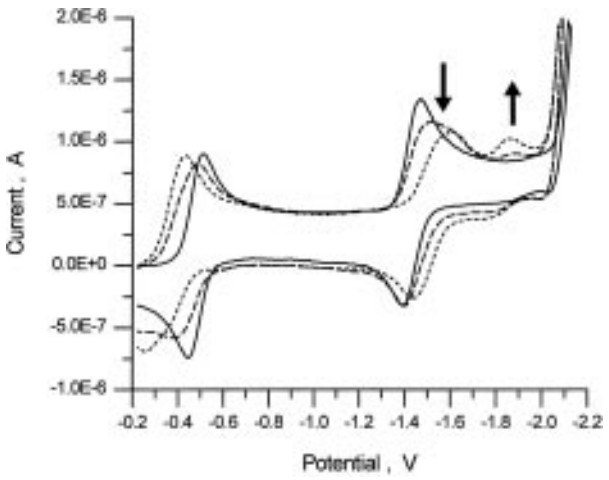

Figure 4. Cyclic voltammograms showing the Fe^{II}/Fe^{I} redox couple of $((2,6\text{-}Cl_2)_4$TPP)$FeClO_4$ (0.5 mM) titrated with pyridine in DMF (0.06 M TBAP): solid line, no ligand; dashed line, [Py] = 5.0×10^{-4} M; dotted line, [Py] = 1.0×10^{-3} M. Sweep window is from −0.2 to −2.2 V (vs Ag/Ag^+), temperature is 25 °C, and scan rate is 50 mV/s. The arrows show the decrease and shift in the cathodic peak near −1.6 V with increase in cathodic peak near −1.9 V that demonstrates the slow kinetics of ligand dissociation from Fe(II).

When the iron porphyrinates are titrated with weakly basic pyridines, especially 4-cyanopyridine, the same slow ligand kinetics observed with the Fe^{II}/Fe^{I} couple are seen with the Fe^{III}/Fe^{II} redox couple as well.[10] With these weakly basic pyridines, there is a large difference in the size of log β_2 for iron(III) and iron(II), ranging from 5−9 orders of magnitude for 4-cyanopyridine to 3−5 orders of magnitude for pyridine. In these titrations, the Fe^{III}/Fe^{II} anodic peak broadens during the middle of the titration, resulting in a peak separation of greater than 70 mV, and then sharpens again at ligand concentrations slightly less than that at which the limiting reduction potential is reached. This behavior is exaggerated in the case of the $((2,6\text{-}Br_2)_4$TPP)-Fe complexed with 4-cyanopyridine, as shown in Figure 5,

(47) Lexa, D. Personal communication.

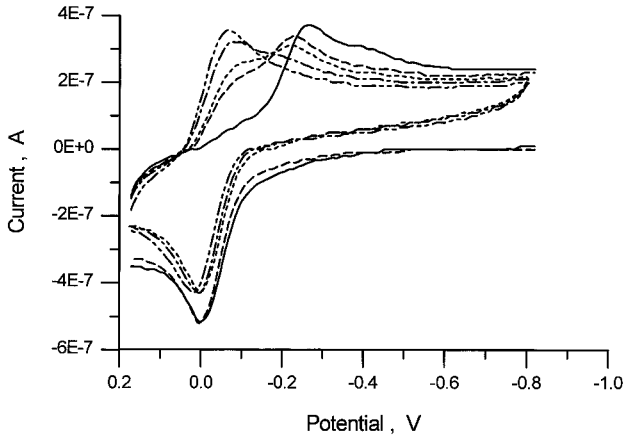

Figure 5. Cyclic voltammograms of the Fe^{III}/Fe^{II} wave for ligand concentrations of 3.5×10^{-2} to 2.5×10^{-1} M for the titration of $((2,6\text{-}Br_2)_4TPP)FeClO_4$ (0.25 mM) with 4-cyanopyridine in DMF (0.03 M TBAP) at 25 °C with a scan rate of 50 mV/s: solid line, [4-CNPy] = 3.5×10^{-2}; progressive changes are for [4-CNPy] = 8.0×10^{-2}, 1.0×10^{-1}, 1.5×10^{-1}, and 2.5×10^{-1} M; at the final concentration (dash−dot−dot line) the Fe^{III}/Fe^{II} wave has regained its symmetrical shape.

where the anodic peak broadens and shifts, sharpens, and then does not shift much further until the cathodic peak "catches up". Then the couple shifts to the final redox potential of the bis(ligand) complex. This behavior is exhibited at scan rates as slow as 10 mV/s. The addition of each axial ligand to the iron(III) center is evident from the changes in the iron(III) reduction peak (Figure 5).

To test the hypothesis that slow ligand exchange is responsible for the observed behavior of the anodic peak of the Fe^{III}/Fe^{II} redox couple, multiple-sweep cyclic voltammograms were recorded on the $((2,6\text{-}Br_2)_4TPP)Fe(4\text{-cyanopyridine})_2$ complex at a ligand concentration such that the cathodic and anodic peaks of the Fe^{III}/Fe^{II} couple were well separated. The resulting voltammograms were identical to one another and to those shown in Figure 5. It is clear that when large peak separations are observed, the iron(III) porphyrinate, with fast ligand exchange, is reduced at the appropriate position for the particular ligand concentration, based upon the value of β_2^{III}, but on the return sweep it is the bisligated iron(II) porphyrinate that is oxidized. Upon oxidation from Fe(II) to Fe(III), the axial ligands dissociate rapidly to leave the iron(III) porphyrinate to be rereduced at the same potential as observed for the first sweep.

By the end of the titrations, the data obtained consisted of the reduction potentials for each redox couple, Fe^{III}/Fe^{II} and Fe^{II}/Fe^{I}, at each ligand concentration. The reduction potentials and the ligand concentrations can be linearly correlated to each other through eq 8 or 9, where $y = (E_{1/2})_c$, $x = \log [L]$, the slope is given by the difference in the number of axial ligands, $(p - q)$, times RT/nF, and the y intercept includes the first two portions of the equation on the right-hand side of eq 8 or 9. Graphical representations of eq 8 utilizing all the data points taken for the titrations of Figures 1−3 are shown below each of the waves in Figures 1−3. In each case, the plot on the left, labeled b, shows the data for the Fe^{III}/Fe^{II} wave and that on the right, labeled c, shows the plot for the Fe^{II}/Fe^{I} anodic peak. For the Fe^{II}/Fe^{I} plot of Figure 1c, the initial portion of the curve has zero slope, indicating $p = 0$ and thus iron(II) is uncoordinated at these ligand concentrations (since iron(I) does not complex ligands at the ligand concentrations and temperature used in the titration). At log [L] more positive than −2.5, the slope becomes approximately −103 mV/decade change in free-ligand concentration, indicating that the slope is approximately $-2(2.303RT/F) = -2 \times 59.1 = -118$ mV, *i.e*, that $p = 2$. Note that the data in this graphical representation are of the anodic peak of the redox couple versus the added ligand concentration, due to the irreversibility of the cathodic peak of the couple. The behavior of the anodic peak appears to be nearly unaffected by the irreversibility of the cathodic peak, since the slope does not deviate greatly from the theoretical 118 mV. Although these data are not thermodynamically valid, they are useful for estimating approximate values of log β_2^{II} and for comparison to those obtained from the Fe^{III}/Fe^{II} redox couple. All values of log β_2^{II} presented in Table 2 were calculated from the ligand concentration behavior of the Fe^{III}/Fe^{II} redox couple, except those marked with asterisks. The systems for which it was necessary to use the values of log β_2^{II} obtained from the behavior of the Fe^{II}/Fe^{I} anodic peak are those for which the values of β_2^{II} and β_2^{III} are very similar, as exemplefied by Figure 3b, and thus only their ratio can be obtained from the Fe^{III}/Fe^{II} wave.

The same analysis can be applied to the plot of the data for the Fe^{III}/Fe^{II} wave of Figure 1b. The initial flat portion of the curve indicates that neither iron(II) nor iron(III) has axial ligands, while between log [pyridine] ∼−2.7 and −1.3, the plot has a positive slope of 113 mV (theoretical value 118 mV), indicating that iron(II) has two axial ligands (as already indicated by the behavior of the Fe^{II}/Fe^{I} wave) and iron(III) has no axial ligands. At log [pyridine] = −0.8, the slope becomes zero once again, indicating that both iron(III) and iron(II) are bisligated. Since the slope never equals ±59 mV for either wave, Fe^{III}/Fe^{II} or Fe^{II}/Fe^{I}, p or q never appears to equal 1. Thus, in this example, only the overall equilibrium constants for the addition of two axial ligands can be determined. However, it was possible to determine the equilibrium constants for addition of one axial ligand for several complexes where K_2 is relatively small compared to K_1, as is discussed below.

The data points used to determine the slope of the $(E_{1/2})_c$ versus log [L] plots are generally those where the ligand concentration is more than 10 times that of the iron porphyrinate ($(0.25-1.0) \times 10^{-3}$ M) and usually at least 10^{-2} M; therefore, the amount of ligand used to form the complex could be ignored, thereby allowing the value of log [L] on the x axis of the plot to be the total amount of ligand added at each point in the titration. Although the difference between total and free ligand concentrations is significant at low ligand concentrations ($10^{-4}-3 \times 10^{-3}$ M), the $(E_{1/2})_c$ versus log [L] plot is usually well-behaved by the point where the ligand concentration is at least 10 times the iron porphyrin concentration.

When "irreversibility" of the Fe^{III}/Fe^{II} wave is observed, the calculation of log β_2^{II} from the Fe^{III}/Fe^{II} data becomes more difficult, because the majority of the points on the sloped portion of the curve are part of this irreversible domain and thus cannot be used for calculations. Fortunately, this peak spreading does not occur immediately and usually ends before the redox couple ceases to shift with further additions of axial ligand. It is in such cases that utilization of the data from the Fe^{II}/Fe^{I} redox couple provides confirmation and, in some cases, the only means of evaluating log β_2^{II}.

The slopes of the plots for the $((2,6\text{-}(OCH_3)_2)_4TPP)Fe$ system were consistently smaller in magnitude than ±100 or ±50 mV, leading to significantly less than integer values of $p - q$. This situation arises when the differences in the equilibrium constants for mono- and bisligation are not large and there are both bis- and monoligated iron porphyrinates of one or both oxidation states present for some portion of the titration. In such cases, analysis using the full expression, eq 7, in which all six possible iron porphyrinate species involved in a particular redox couple are considered, is required. Because it cannot be linearized, a

Table 2. Equilibrium Constants for Bis(ligand) Complex Formation with Iron(II) Tetraphenylporphyrinates in Dimethylformamide

		log β_2^{II} of ((2,6-X_2)$_4$TPP)Fe					
axial ligand	pK_a(BH$^+$)	Br	Cl	CH_3	F	H	OCH_3
4-CNPy	~1.1	9.1 ± 0.5	8.0 ± 0.2	7.5 ± 0.1	6.0 ± 0.6	5.6 ± 0.4	6.6 ± 0.1
pyridine	5.22	9.4 ± 0.2	8.2 ± 0.2	7.4 ± 0.4	6.6 ± 0.3	5.7 ± 0.2	5.8 ± 0.1
3,4-Me_2Py	6.46	8.9 ± 0.3	7.8 ± 0.4	7.3 ± 0.4	7.0 ± 0.2	5.6 ± 0.2	5.1 ± 0.1
4-NMe_2Py	9.7	>9[a]	8.4[a] ± 0.2	7.9[a] ± 0.4	7.2 ± 0.8	6.7[a] ± 0.1	5.8 ± 0.1
N-MeIm	7.33	7.7* ± 0.5	7.4[a] ± 0.2	7.3[a] ± 1.1	6.9 ± 0.5	6.5 ± 0.2	4.9 ± 0.2
2-MeImH	7.56	5.2 ± 0.2	5.6 ± 0.2	5.5 ± 0.5			

[a] Estimated from Fe^{II}/Fe^{I} cathodic peak shift (see text).

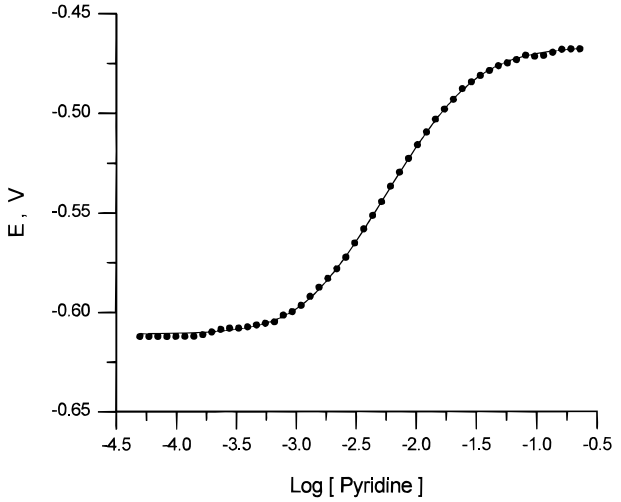

Figure 6. Actual $(E_{1/2})_c$ (filled circles) versus log [L] data and the curve fit to eq 8 (solid line) for ((2,6-$(OCH_3)_2$)$_4$TPP)$FeClO_4$ titrated with pyridine.

curve-fitting program that employs least-squares minimization of the fit of the experimental data to eq 7 was used. An example of one such fit is shown in Figure 6. Such curve fitting was necessary for all titrations of ((2,6-$(OCH_3)_2$)$_4$TPP)Fe and for some titrations of other iron porphyrinates with weaker bases, where a plateau was never achieved in the $(E_{1/2})_c$ versus log [L] plots. In some cases, it was found that while one oxidation state of the iron porphyrinate clearly showed stepwise addition of axial ligands, with $K_1 \sim K_2$, the other oxidation state did not appear to add ligands in a stepwise fashion. In these cases, the "apparent" stepwise constant K_1 was much smaller than K_2 (as calculated from $K_2 = \beta_2/K_1$) and is considered unreliable. This is observed for logK_1^{III} of the 4-cyano-, 3,4-dimethyl-, and 4-(dimethylamino)pyridine complexes of (2,6-$(OCH_3)_2$)$_4$(TPP)-Fe^{III} and for log K_1^{II} of the *N*-methylimidazole complex of the Fe(II) form of the same porphyrinate (Table 4). For consistency, curve fitting was carried out on all titration data. However, it was found that for titrations of the higher-basicity ligands with all iron porphyrinates except ((2,6-$(OCH_3)_2$)$_4$TPP)Fe, in the vast majority of these cases the values of log K_1^{III} and log K_1^{II} obtained from the fits were very small compared to the expected error limits, and the values of log β_2^{III} and log β_2^{II} obtained were very similar to those estimated utilizing eq 8.

Finally, the magnitude of the equilibrium constants for bisligation of iron(III) were estimated by UV−visible spectrophotometry without supporting electrolyte for three complexes, ((2,6-Br_2)$_4$TPP)$FeClO_4$ with pyridine and ((2,6-$(OCH_3)_2$)$_4$TPP)-$FeClO_4$ with pyridine and 3,4-lutidine.[4] The actual constants were not calculated from the data obtained since clear isosbestic points were not observed, indicating the presence of more than two species in the solutions during the majority of the titration, as was observed in the electrochemical studies. One of the additional species present was probably the 1:1 complex, while another appeared to be the iron(II) complex, presumably formed by large-scale autoreduction of the iron(III) complex by the added ligand. From the amount of ligand used to achieve the apparent half-conversion to biscoordination of the iron(III) center, the magnitudes of the equilibrium constants were estimated and are quite consistent with the electrochemically-measured values. The values of log β_2^{III} approximated in this way are 5.7 for ((2,6-Br_2)$_4$TPP)$FeClO_4$ with pyridine, and 3.2 and 3.6 for ((2,6-$(OCH_3)_2$)$_4$TPP)$FeClO_4$ with pyridine and 3,4-lutidine, respectively. These values are similar to those determined electrochemically, as summarized in Table 3.

Reduction Potentials of All Iron Porphyrinates. The half-wave potentials of the Fe^{III}/Fe^{II} and Fe^{II}/Fe^{I} oxidation/reduction couples without ligand and for the Fe^{III}/Fe^{II} oxidation/reduction couples at the end of the titration for each of the five iron porphyrinates utilized in this study are shown in Table 1. The ordering of the initial reduction potentials for both the Fe^{III}/Fe^{II} and Fe^{II}/Fe^{I} couples in the order of most easily reduced to most difficult is 2,6-F_2 > 2,6-Cl_2 > 2,6-Br_2 > TPP(H) > TMP-($(CH_3)_3$) > 2,6-$(OCH_3)_2$. This approximately (except for fluoro) follows the order of electron-donating/electron-withdrawing capabilities of the substituents,[48] as has been shown previously with phenyl *meta* and *para* substituents.[2,4,9] It is interesting to note that although the tetraphenylporphyrinate complexes of this study contain phenyl *ortho* substituents, the observed trend of reduction potentials is close to that expected on the basis of values of the *para* Hammett σ constants.[48] However, this apparently simple behavior is not observed for the equilibrium constants, as will be discussed below.

The same general trend in the Fe^{III}/Fe^{II} reduction potentials is observed at the end of the titration where the both iron(III) and iron(II) are biscomplexed. The only discrepancy in the order is with (TPP)Fe and its 4-cyanopyridine complex, although the (TPP)Fe/4-cyanopyridine reduction potential is in accord with the equilibrium constants to be discussed in the next section and presented in Tables 2 and 3, where the constants for both iron(II) and iron(III) with 4-cyanopyridine are somewhat larger than expected. Final potentials for the 2-methylimidazole complexes are not given for (TPP)Fe^{II}, (2,6-$(OCH_3)_2$)$_4$(TPP)-Fe^{II}, and (2,6-F_2)$_4$(TPP)Fe^{II}, since these iron(II) porphyrinates do not form detectable amounts of bis complexes at concentrations of 2-methylimidazole less than 1 M.

The observed trends in initial and final potentials, based upon the electronic effects of substituents, no longer hold when the differences in potential, $\Delta E_{1/2} = E_{1/2}$(fully complexed) − $E_{1/2}$(uncomplexed), are considered. The value of $\Delta E_{1/2}$ is a reflection of the ratio of the equilibrium constants for biscoordinated iron(III) and iron(II), and a positive change indicates that iron(II) has the larger equilibrium constant while a negative change indicates that iron(III) has the larger constant. A near-zero change indicates nearly identical equilibrium constants for the two oxidation states. The observed trend in $\Delta E_{1/2}$ indicates that stronger σ donors stabilize the iron(III) complexes more than the iron(II) complexes, as will be discussed further below.

(48) Hansch, C.; Taft, R. W. *Chem. Rev.* **1991**, *91*, 165.

Table 3. Equilibrium Constants for Bis(ligand) Complex Formation with Iron(III) Tetraphenylporphyrinates in Dimethylformamide

		log β_2^{III} of ((2,6-X_2)$_4$TPP)Fe					
axial ligand	pK_a(BH^+)	Br	Cl	CH_3	F	H	OCH_3
4-CNPy	~1	0.8 ± 0.4	−0.2 ± 0.1	0.2 ± 0.1	<−0.2	<−0.8	−0.2 ± 0.1
pyridine	5.22	5.0 ± 0.1	3.8 ± 0.1	3.3 ± 0.3	1.3 ± 0.3	2.2 ± 0.02	3.2 ± 0.2
3,4-Me_2Py	6.46	5.8 ± 0.3	4.3 ± 0.4	4.4 ± 0.3	2.7 ± .2	2.4 ± 0.01	4.0 ± 0.1
4-NMe_2Py	9.7	>9[a]	8.4[a] ± 0.2	8.3[a] ± 0.4	6.3 ± 0.8	6.8[a] ± 0.1	7.5 ± 0.2
N-MeIm	7.33	7.7[a] ± 0.6	7.1[a] ± 0.2	7.9[a] ± 1.1	6.2 ± 0.5	7.2 ± 0.3	7.0 ± 0.2
2-MeIm	7.56	6.7 ± 0.02	7.3 ± 0.1	7.4 ± 0.5	5.6 ± 0.1	5.2 ± 0.02	5.9 ± 0.1

[a] Estimated from Fe^{II}/Fe^{I} cathodic peak shift (see text).

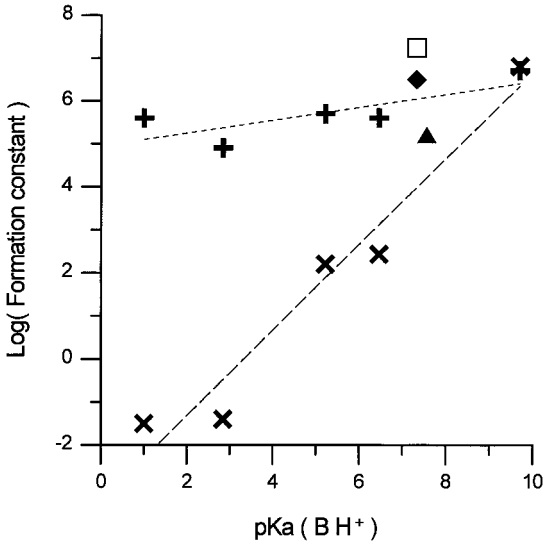

Figure 7. Plot of log β_2^{II} and log β_2^{III} for the iron tetraphenylporphyrinate complexes of this study versus the basicity of the axial ligands, expressed as pK_a(BH^+): +, substituted pyridines, Fe(II); ×, substituted pyridines, Fe(III); □, *N*-MeIm, Fe(II); ◆, *N*-MeIm, Fe(III); ▲, 2-MeImH, Fe(III). Dashed lines represent the least-squares linear correlations for the substituted pyridine complexes of Fe(II) and Fe(III).

Equilibrium Constants for Axial Ligand Complexes with the Parent Compound, Iron Tetraphenylporphyrinate. The equilibrium constants for all complexes are shown as log β_2^{II} in Table 2 for Fe(II) and logB_2III in Table 3 for Fe(III). For the parent (tetraphenylporphyrinato)iron complexes, a steady trend in increasing size of the constants is observed for the pyridine complexes with the least basic pyridines having the smallest equilibrium constants, a trend noted in earlier studies.[4,33] A graphical representation of log β_2 vs pK_a(PyH^+) for (TPP)-Fe^{III} and -(II) is shown in Figure 7; the linearity, except for the 4-cyanopyridine complex, is quite evident in these plots with a slope of 1.0 for log β_2^{III} and 0.15 for log β_2^{II}. The linearity with the pK_a of the conjugate acid of each of the pyridines suggests a purely σ interaction between the pyridines and the iron center, although there may also be a π interaction that contributes linearly with the σ interaction, since the energies of both the π and σ filled orbitals of the pyridine vary linearly with the pK_a of the conjugate acid of the pyridine.[49]

There is a much stronger dependence of the equilibrium constants on the basicity of the substituted pyridine for the iron-(III) complexes than for the iron(II) complexes. This difference may be due to the overall charge of the complexes, since the Fe(III) center carries a formal positive charge, both when complexed with DMF and after complexation of the axial ligands, while the Fe(II) center does not. Both the σ- and π-donating abilities of the pyridine contribute to neutralizing the net positive charge, and for the more basic pyridines, which are both strong σ and π donors, the binding is strongly enhanced. The dependence of log β_2^{II} on axial ligand basicity is much less than that for log β_2^{III}, since there is no longer a net positive charge on the iron. Nevertheless, all equilibrium constants for Fe(II) are significantly larger than or equal to those for Fe(III). On the basis of charge alone, one would have expected the opposite. However, (TPP)Fe^{II} has larger equilibrium constants for addition of axial ligands than does (TPP)Fe^{III}, in part because the number of DMF molecules on Fe(III) differs from that of Fe(II): Iron(III) is known to be coordinated to two DMF molecules,[37,50] while iron(II) is coordinated to only one.[37] Thus, it is likely that the enthalpy of formation of the bis(ligand) complexes contributes significantly to the large size (and more than compensates for the unfavorable entropy term for addition of a second axial ligand) of the iron(II) equilibrium constants. The similar magnitude of all log β_2^{II} values for a given iron porphyrinate suggests that ΔH remains fairly constant for iron-(II) biscomplex formation for all axial ligands.

The results of this study (Tables 2 and 3) compare well to most literature values summarized elsewhere,[27] with expected differences where the data were obtained in other solvents or with other anions. However, the values for log β_2^{II} and log β_2^{III} for the (TPP)Fe complexes obtained in this study, Tables 2 and 3, are significantly different (by up to 9 orders of magnitude smaller) from those reported by Bottomley and Kadish.[33] The only apparent difference between the two studies is the solvent, DMF in this study and methylene chloride in the Bottomley and Kadish study. Because DMF is a coordinating solvent,[37,50] the equilibrium constants reported herein are actually ligand exchange constants, while those reported previously[33] may be true formation constants. If the binding of DMF and the resulting exchange constants are considered, the equilibrium constants measured in this study would differ by the factor of the equilibrium constant for the addition of the appropriate number of DMF solvent molecules to the iron centers in the two oxidation states, a *constant* for a given iron porphyrinate. However, the difference is not constant, but rather varies from 3.4 to 9.5 orders of magnitude for β_2^{II} and from 1.4 to 3.0 orders of magnitude for β_2^{III}. Thus, replacement of coordinated DMF cannot account for the large range of differences between the (TPP)Fe^{II} equilibrium constants reported herein and those reported by Bottomley and Kadish.[33] We cannot account for the large discrepancies between the two sets of data, but we are confident of our measurements and note that the log β_2^{III} values for 4-(dimethylamino)pyridine and *N*-methylimidazole reported herein are very similar, as they also are in the earlier study reported from this laboratory, in which β_2^{III} values were measured in chloroform by spectrophotometric techniques.[4]

Equilibrium Constants for Axial Ligand Complexes of "Hindered" Iron Tetraphenylporphyrinates. It has been shown by many workers, including ourselves, that many physical properties of metallotetraphenylporphyrinates having

(49) (a) Ramsey, B. G.; Walker, F. A. *J. Am. Chem. Soc.* **1974**, *96*, 3314. (b) Lichtenberger, D. L.; Walker, F. A.; Gruhn, N. E.; Bjerke, K. J. To be submitted.

(50) Zobrist, M.; La Mar, G. N. *J. Am. Chem. Soc.* **1978**, *100*, 1944.

either *meta* or *para* substituents on the phenyl rings are correlated with the Hammett σ constants of the substituents:[2−15]

$$P(\mathrm{X}) - P(\mathrm{H}) = 4\sigma_{\mathrm{X}}\rho \qquad (10)$$

where P(X) and P(H) are the observed physical property of the tetraphenylporphyrins having substituents X and H, respectively, σ_{X} is the Hammett substituent constant of X, and ρ describes the sensitivity of the property being studied to the electron-withdrawing or -donating properties of X.[48,51] These linear free energy relationships have been useful in understanding the electronic effects of the *meta* or *para* substituents on the reactivity of the free-base porphyrins or metalloporphyrinates. Earlier studies that examined the effects of electron-donating or -withdrawing substituents on the phenyl rings of a series of (tetrakis(substituted phenyl)porphyrinato)metal(II) complexes in benzene or toluene solution on the size of the equilibrium constants for axial ligand complexes of Ni(II),[3a] $(VO)^{2+}$,[3a] Co(II),[3b−d] and Zn(II),[6,7] showed that the ρ values were positive in all cases. Kadish and Bottomley measured the iron(II) equilibrium constants for the same complexes used by Walker *et al.* for the iron(III) study[4] and found ρ to be +0.13,[10] a positive value as with other uncharged metalloporphyrinates.[3,6,7] This has been called the "Lewis acid contribution",[4] and it arises from a decrease or an increase in Lewis acidity of the metal center in response to the electron-donating or electron-withdrawing abilities of the phenyl substituents. In contrast, for iron(III) porphyrinates in chloroform or dichloromethane solution, binding of two neutrally-charged ligands to the metal creates a net positive charge on iron(III) in the product by displacement of the bound chloride ion in these solvents.[2,4] This contribution from charge separation creates the opposite dependence, and a value of $\rho = -0.39$ was reported, indicating that electron-donating groups favor the formation of the complex.[4] An estimation of the charge separation contribution for these iron(III) tetraphenylporphyrinates was based upon the ρ value for the Ni(II) series ($\rho = +0.33$).[3a] The combination of the charge and Lewis acid contributions thus led to a predicted ρ_{charge} of ~ -0.7 for the charged Fe(III) center.[4] Later, Brewer and Brewer[29] determined the equilibrium constants for the same set of *para*-substituted (tetraphenylporphyrinato)iron(III) chlorides with *N*-methylimidazole in DMSO and found that $\rho = +0.11$.[29] DMSO is a coordinating solvent[50] whereas chloroform is not, and the charge stabilization was observed by Walker *et al.*[2,4] This value of ρ suggests that the charge contribution is actually smaller ($\rho_{\mathrm{charge}} \sim -0.5$) than estimated previously.[4] For the systems studied in the present work in DMF, we should expect a positive ρ for the iron(III) equilibrium constants, since DMF, like DMSO, is a coordinating solvent.[50] Hammett σ constants have not been reported for *ortho* substituents, but if *para* substituent constants, σ_{p} (Br = Cl = +0.23 > F = +0.06 > H = 0 > CH_3 = −0.17 > OCH_3 = −0.27[48]), are used as a measure of the electron-donating or -withdrawing characteristics of the *ortho* substituents used in this study, it is apparent that the equilibrium constants do not follow this trend, since log β_2^{III} is larger for the $((2,6\text{-}Br_2)_4\mathrm{TPP})\mathrm{Fe}$ complexes than for the dichloro analogs, even though the corresponding Hammett σ_{p} constants are identical, and (TMP)Fe complexes have equilibrium constants similar to those of the $((2,6\text{-}Cl_2)_4\mathrm{TPP})\mathrm{Fe}$ complexes, even though the σ_{p} values are approximately equal in magnitude but opposite in sign.

The equilibrium constants for each of the axial ligand complexes of the series of iron(II) porphyrinates only roughly follow the Hammett σ constants for phenyl *para* substituents.[48] The values of σ_{p} at least approximately follow the sizes of log β_2, particularly for the iron(II) complexes of a given axial ligand (Table 2), and would indicate a negative value of ρ. However, it is expected that Fe(II) should behave as the other +2 metals and have a *positive* value of ρ. Thus, the equilibrium constants for the axial ligand complexes of hindered tetraphenylporphyrinates of both Fe(II) and Fe(III) do not appear to follow the expected linear free energy trends expected for *para*-substituted tetraphenylporphyrinates.

The trends in the sizes of equilibrium constants for hindered iron porphyrinates reported in Tables 2 and 3 appear to follow the *size* of the *ortho* substituents more closely than the Hammett σ_{p} constants. The measured van der Waals radii (in Å) of the ortho substituents are CH_3 = ∼2.0,[52] Br = 1.90,[53] Cl = 1.80,[53] OCH_3 ∼1.4 (with the methyl group rotated away from the axial ligand),[52] F = 1.35,[53] and H = 1.20.[53] As reported for one case previously,[54] complexes having larger *ortho* substituents generally have larger log β_2^{III} values; in the present study we find that log β_2^{III} varies in the order Br > Cl > CH_3 > OCH_3 > H > F. Thus, for iron(III), the decreasing size of log β_2^{III} almost exclusively follows the trend in decreasing size, provided that the methyl group of the methoxy substituent rotates away from the core of the porphyrin to minimize steric interaction with the axial ligand. For the iron(III) porphyrinates, where the necessity of stabilizing the formal positive charge creates a strong electron demand,[2] it is also possible that the electron cloud of the larger substituents may overlap with the π cloud of the porphyrinate ring. This overlap could cause a through-space increase in the electron density at the iron(III) center that could aid in stabilizing the net positive charge in the bis(ligand) complex. This increase in electron density would, however, decrease the Lewis acidity of the metal, and in the iron(II) case would serve to decrease, rather than increase, the size of the equilibrium constants. In spite of this, only a slightly different trend is found for log β_2^{II}: Br > Cl > CH_3 > F > H > OCH_3.

It is also possible that a structural stabilization factor may arise from the fact that bulkier substituents may cause more extreme S_4 ruffling of the Fe(III) porphyrinates. Except for one report of the molecular structure of $[((2,6\text{-}Cl_2)_4\mathrm{TPP})\mathrm{Fe}(1\text{-vinylimidazole})_2]ClO_4$,[54] only the structures of TMP and TPP complexes have been reported.[16−18,56] Among these, it is found that for $[(\mathrm{TMP})\mathrm{FeL}_2]^+$, where L = *N*-methylimidazole, the ligands are in parallel planes and the porphyrinate ring is not ruffled,[16] while for L = pyridines of all basicities, the ligands are in perpendicular planes and the porphyrinate rings are significantly and similarly ruffled in every case,[16,17] and when L = 1,2-dimethylimidazole, the ligands are again in perpendicular planes and the porphyrinate core is more ruffled than for any other Fe(III) porphyrinate reported thus far.[18] However, at least for pyridine ligands, the degree of ruffling is not necessarily a result of the bulkiness of the phenyl 2,6 substituents but rather arises in large part from electronic factors, as is evidenced by the highly ruffled structure of $[(\mathrm{TPP})\mathrm{Fe}(4\text{-cyanopyridine})_2]^+ClO_4^-$, for which there is no *steric* reason for ruffling.[55] And while ruffling *may* help to stabilize iron(III) porphyrinate complexes, the iron(II) counterparts are *not*

(51) Hammett, L. P. *Trans. Faraday Soc.* **1938**, *34*, 156.
(52) Streitwieser, A.; Heathcock, C. H. *Introduction to Organic Chemistry*, 2nd ed.; Macmillan: New York, 1981; p 148.
(53) Huheey, J. E. *Inorganic Chemistry*, 3rd ed.; Harper & Row: New York, 1983.
(54) Hatano, K.; Safo, M. K.; Walker, F. A.; Scheidt, W. R. *Inorg. Chem.* **1991**, *30*, 1643.
(55) Safo, M. K.; Walker, F. A.; Raitsimring, A. R.; Walters, W. P.; Dolata, D. P.; Debrunner, P. G.; Scheidt, W. R. *J. Am. Chem. Soc.* **1994**, *116*, 7760.
(56) Safo, M. K.; Nesset, M. J. M.; Walker, F. A.; Debrunner, P. G.; Scheidt, W. R. Manuscript in preparation.

ruffled,[56] except, we suspect, for the bis(2-methylimidazole) or bis(1,2-dimethylimidazole) complexes, for which structures have not yet been obtained. In addition, the same trend in equilibrium constants is shown in the reactions of *N*-methylimidazole with a series of unsymmetrically substituted (tetraphenylporphyrinato)iron(III) chlorides, where the same *ortho* substituents as used in this study were present on only one of the phenyl rings, while *para*-methoxy groups were located on the other three phenyl rings.[31] (In this case the degree of ruffling is not expected to depend upon the size of the *ortho* substituents on the single phenyl ring, since only one ring carries these substituents.) The values of log β_2^{III} for the series of (mono-(2,6-X_2 phenyl)porphyrinato)iron(III) and (tris(*p*-methoxyphenyl)(porphyrinato)iron(III)[31] and their similarity to the trends observed herein point to the possibility of a through-space overlap of the electron cloud of the substituent with the π-electron cloud of the porphyrinate ring that creates a stronger electron-donating effect as the size of the substituent increases.[31]

One might expect the degree of general solvation, as distinct from solvent coordination to the metal, to play a role in the ability of the iron center to coordinate axial ligands. The least solvated iron center should have the largest equilibrium constants, as suggested previously for the picket fence porphyrin.[57] This line of reasoning is consistent with the observation that the bulkiest systems studied, ((2,6-Br_2)$_4$TPP)Fe^{III} and -Fe^{II}, have the largest equilibrium constants. However, steric restriction of the solvent should equally well restrict the approach of the larger imidazole and pyridine ligands, which is not in accord with the results. Therefore, we do not believe that the degree of nonspecific solvation plays a large role in determining the sizes of the equilibrium constants. This lack of steric protection from solvation affecting coordination of neutral axial ligands was also seen by Lexa and Savéant for a series of basket-handle (porphyrinato)iron(II) complexes.[37] Walker and Benson observed the same effect for a series of Zn(II) porphyrinates, where a bulky *ortho* substituent actually led to an *increase* in the size of the equilibrium constant.[58]

As is the case for the TPP complexes discussed above, log β_2^{III} values for the hindered (tetraphenylporphyrinato)iron(III) complexes vary linearly with the pK_a of the conjugate acid of the pyridine ligand, as shown in Figure 8 and supporting Figures S1−S4. The slopes of the correlations are 0.9 (CH_3 (TMP)), 1.0 (Br, Cl), 0.8 (F), and 0.9 (OCH_3). In contrast, none of the hindered iron(II) porphyrinate complexes show a dependence upon the base strength of the pyridines studied, within experimental error (see Table 2 and Figure 8); *i.e.*, the reactivity of the bases is "leveled". It should be noted that log β_2^{II} is "leveled" to a unique value for each iron porphyrinate, suggesting a different inherent Lewis acidity for each iron(II) porphyrinate. As mentioned, the unique value of log β_2^{II} for each of the 2,6-disubstituted phenyl derivatives of (TPP)Fe^{II} appears to increase with increasing size of the *ortho* substituent.

The complexes for which log K_1 values could be determined are listed in Table 4. As stated earlier, stepwise equilibrium constants were determined for several of the iron tetrakis(2,6-dimethoxyphenyl)porphyrinates, as well as for several other systems for which the slope of the Fe^{III}/Fe^{II} potential vs log [L] deviated from ±118 mV. However, in cases where the deviation was less than ±10 mV, no unique value of log K_1^{II} or log K_1^{III} could be obtained, and only the overall log β_2^{II} and log β_2^{III} could be obtained from the fits. It is interesting to note the similarity in magnitude of log K_1^{II} for mono(pyridine) complexes of iron(II); as for the case of log β_2^{II}, these values appear to be "leveled".

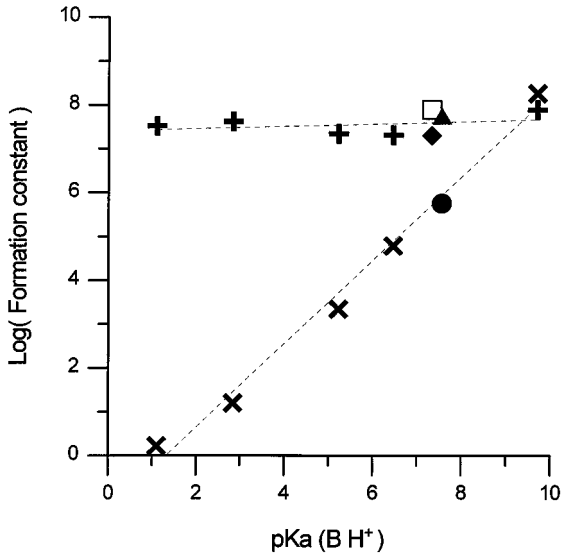

Figure 8. Plot of log β_2^{II} and log β_2^{III} for the iron tetramesitylporphyrinate complexes of this study versus the basicity of the axial ligands, expressed as pK_a(BH^+): +, substituted pyridines, Fe(II); ×, substituted pyridines, Fe(III); □, *N*-MeIm, Fe(II); ◆, *N*-MeIm, Fe(III); ●, 2-MeImH, Fe(II); ▲, 2-MeImH, Fe(III). Dashed lines represent the least-squares linear correlations for the substituted pyridine complexes of Fe(II) and Fe(III).

Table 4. Stepwise Formation Constants for Iron(II) and Iron(III) Tetraphenylporphyrinates at 25 °C

ligand	log K_1^{II}	log K_2^{II} [a]	log K_1^{III}	log K_2^{III} [a]
		((2,6-(OMe)2)4TPP)Fe		
4-CNPy	2.3 ± 0.7	4.3	−0.1 ± 0.4[b]	(−0.1)[c]
Py	2.2 ± 0.1	3.6	1.5 ± 0.3	1.7
3,4-Me_2Py	2.6 ± 0.2	2.5	0.2 ± 0.9[b]	(3.8)[c]
4-NMe_2Py	2.9 ± 0.6	2.9	0.7 ± 0.7[b]	(6.8)[c]
N-MeIm	1.3 ± 1.2[b]	(3.6)[c]	3.3 ± 0.2	3.7
2-MeImH	3.2 ± 0.1		2.6 ± 0.2	3.3
		(TPP)Fe		
2-MeImH	3.4 ± 0.1		3.1 ± 0.2	2.1
		(TMP)Fe		
N-MeIm	5.1 ± 1.3	2.2		
2-MeImH	3.6 ± 0.2	1.9		

[a] Calculated from log β_2^{II} − log K_1^{II} or log β_2^{III} − log K_1^{III}. [b] Apparent best fit value. [c] Apparent value, based on apparent log K_1^{II} or log K_1^{III}.

Comparison of Imidazoles to Pyridines. In this study we have reached the same conclusions as have previous studies of metal porphyrinate complexes with imidazoles and pyridines,[4,5] that imidazoles behave differently than pyridines, with respect to both the reduction potentials (Table 1) and equilibrium constants (Tables 2 and 3, Figures 7 and 8, and supporting Figures S1−S4). Beginning with the final reduction potentials for the Fe^{III}/Fe^{II} couple, both the imidazoles form bis complexes that are harder to reduce ($E_{1/2}$ more negative) than those of any of the pyridines and in fact are harder to reduce than the free iron porphyrinate itself. This indicates that log β_2^{III} is larger than log β_2^{II} for both 2-methylimidazole and *N*-methylimidazole complexes, while for all pyridine complexes, log $\beta_2^{II} \geq$ log β_2^{III}. The 2-methylimidazole complexes have the most cathodic reduction potentials of any bis(ligand) complexes investigated for the three iron porphyrinates with which it fully forms six-coordinate complexes in both oxidation states, *i.e.* ((2,6-Br_2)$_4$-TPP)Fe, ((2,6-Cl_2)$_4$TPP)Fe, and (TMP)Fe. Additionally, the

(57) Collman, J. P. *Acc. Chem. Res.* **1977**, *10*, 265.
(58) Walker, F. A.; Benson, M. *J. Am. Chem. Soc.* **1980**, *102*, 5530.
(59) Albert, A. *Phys. Methods Heterocycl. Chem.* **1963**, *1*; **1971**, *3*.

imidazoles have pK_a(BH^+) values that are smaller, 7.33[59] and 7.56 (corrected for the presence of two protons in the conjugate acid)[59] for *N*-MeIm and 2-MeImH, respectively, than for 4-NMe_2Py, yet they stabilize the iron center more, indicating a much greater inherent base strength toward the metal. Presumably the stabilization comes from π-orbital interactions with the iron center and/or the inherently less steric hindrance to binding to the iron porphyrinate of a five-membered imidazole than of a six-membered pyridine ring and/or more complete stabilization of the $(d_{xy})^2(d_{xy},d_{xz})^3$ ground state than for the lower-basicity pyridines. It should be noted, however, that log β_2^{III} and log β_2^{II} are very similar for 4-NMe_2Py and the imidazoles. Only the equilibrium constants of the *N*-methylimidazole complexes can be directly compared to those of the pyridine complexes, since 2-MeImH has a severe steric constraint which is expected to affect complex formation in a unique way. In fact, up to a concentration of 2 M ligand, 2-MeImH does not form bis(ligand) complexes with (TPP)Fe^{II}, ((2,6-F_2)$_4$(TPP)Fe^{II}, and ((2,6-(OCH_3)$_2$)$_4$TPP)Fe^{II} at 25 °C (Table 4).

While both imidazoles have larger equilibrium constants with iron porphyrinates having larger *ortho* substituents than do the pyridines, 2-methylimidazole only forms biscoordinated iron(II) complexes with iron porphyrinates having larger substituents (bromine, chlorine, and methyl), and only monocoordinated complexes with those having smaller substituents (hydrogen, fluorine, and methoxy). When comparing the log K_1^{II} values of the monosubstituted complexes, they are relatively similar in magnitude and larger than the log K_2^{II} of the bis-2-MeImH complexes, some of which are too small to measure. However, the overall constants, log β_2^{II}, are very different from one another. When 2-methylimidazole coordinates, it must do so in an orientation that allows room for the 2-methyl substituent. The porphyrinate is forced to accommodate by ruffling. As stated previously, X-ray crystallographic data have shown that while the iron(III) complexes of the hindered porphyrinates have S_4-ruffled structures, the iron(II) complexes are planar,[56] although it is unlikely that this would be possible for 2-methylimidazole. It is interesting that the most sterically hindered iron(II) porphyrinates form the most stable complexes with 2-MeImH and that the equilibrium constants are large enough to ensure biscoordination of this ligand at ambient temperatures in the presence of only a 10^{-2} M concentration of free ligand. It would appear, therefore, that bulky phenyl *meso* substituents "encourage" the porphyrinate ring to ruffle and thereby help to stabilize the complexes of both Fe(III) and Fe(II) porphyrinates with bulky ligands. The Mössbauer spectra of [(TMP)Fe(2-MeImH)$_2$] and [(TMP)Fe(1,2-Me_2Im)$_2$][60] and the ^{1}H NMR spectrum of the latter[61] have been observed, and it should be possible to grow single crystals of these or related complexes. Such efforts are underway in our laboratory.

For *N*-methylimidazole, the equilibrium constants for bis complexes of both oxidation states are quite similar. The similarity of log β_2^{III} and log β_2^{II} is a very good situation with respect to the biological role of bis(histidine)-coordinated hemes in electron transfer. The values of log β_2^{III} and log β_2^{II} for *N*-methylimidazole indicate that, regardless of the oxidation state of iron, the coordination should remain unchanged. Except for 4-(dimethylamino)pyridine, this is in sharp contrast to the situation for the pyridines, where log β_2^{III} < log β_2^{II}. However, more careful comparison of these model hemes to the bis(histidine)-coordinated cytochromes points out that *N*-methylimidazole cannot participate in hydrogen-bonding to anions[4] or Lewis bases,[62] as could histidine, and thus hydrogen-bonding could provide an added stabilization of the Fe(III) state by at least 3 orders of magnitude due to delocalization of the positive charge on the iron(III),[4] although the same would not be expected to be true for iron(II). Assuming a direct correlation to the proteins' coordination of the heme, log β_2^{III} could be larger than 10. Furthermore, the histidine imidazole rings in the proteins are held in fixed orientation through hydrogen-bonding to amino acid side chains or the protein backbone and are presented to the metal at a correct distance and geometry to allow coordination. This is expected to give rise to a favorable entropy term and may lead to even larger equilibrium constants than those determined here.

Comparison of these findings concerning model hemes to the axial ligand stabilities of heme proteins reveals a variety of different behaviors and several interesting points. The first of these is that for cytochrome b_5, in which the heme iron is bound to two histidine ligands, the process of "heme rotation", whereby the non-covalently-attached protohemin dissociates from and reassociates with the protein to form the stable ratio of heme rotational isomers, has a half-life of 12 h in the presence of 0.1 M electrolyte[63] or significantly longer (21.5 h) in its absence,[64] whereas heme rotation in the *reduced* protein ferrocytochrome b_5 is at least 100 times slower.[64] Rates of the overall process of ligand loss, heme dissociation, heme reassociation, and ligand binding are not necessarily directly related to equilibrium constants for histidine coordination because a number of steps are involved. However, for the coordination process alone, where ligand binding is expected to be diffusion controlled, the equilibrium constant should be inversely proportional to the rate constant for ligand dissociation. *If* this (small) rate of ligand dissociation is the rate-determining step for heme rotation, then the much faster rate of heme rotation for ferri- than for ferrocytochrome b_5 would suggest that $\beta_2^{II} \gg \beta_2^{III}$ for histidine binding to iron in the two oxidation states. The same conclusion can be reached with regard to methionine binding to a number of ferri- and ferrocytochromes *c*, on the basis of equilibrium constants for displacement of the methionine ligand by imidazole and other ligands,[65] the ease of denaturation of the protein with urea or guanidinium chloride,[65d,66] and hydrogen−deuterium exchange rates of amide protons.[67] In sharp contrast to these observations is the finding that the bis(histidine)-coordinated heme of cytochrome *c*″ from *Methylophilus methylotrophus* readily loses one of its histidine ligands to become a high-spin Fe(II) center upon reduction,[68] thus indicating that $\beta_2^{II} \ll \beta_2^{III}$ in this case. This loss of a histidine ligand is coupled to a redox-linked proton transfer reaction, and it is believed that the site of protonation is the released histidine nitrogen.[69] Why this

(60) Polam, J. R.; Wright, J. L.; Christensen, K. A.; Walker, F. A.; Flint, H.; Winkler, H.; Grodzicki, M.; Trautwein, A. X. *J. Am. Chem. Soc.* **1996**, *118*, 5272.
(61) Polam, J. R.; Shokhireva, T. Kh.; Walker, F. A. To be submitted.
(62) Doeff, M. M.; Sweigart, D. A.; O'Brien, P. *Inorg. Chem.* **1983**, *22*, 851.
(63) Walker, F. A.; Emrick, D.; Rivera, J. E.; Hanquet, B. J.; Buttlaire, D. H. *J. Am. Chem. Soc.* **1988**, *110*, 6234.
(64) McLachlan, S. J.; La Mar, G. N.; Burns, P. D.; Smith, K. M.; Langry, K. C. *Biochim. Biophys. Acta* **1986**, *874*, 274.
(65) (a) Schejter, A.; Aviram, I. *Biochemistry* **1972**, *8*, 149. (b) Sutin, N.; Yandell, J. K. *J. Biol. Chem.* **1972**, *247*, 6932. (c) Morishima, I.; Ogawa, S.; Yonezawa, T.; Iizuka, T. *Biochim. Biophys. Acta* **1978**, *532*, 48. (d) Holt, J. M.; Meyer, T. E.; Axelrod, H.; Cusanovich, M. A. To be submitted.
(66) (a) Knapp, J. A.; Pace, C. N. *Biochemistry* **1974**, *13*, 1289. (b) Cohen, D. S.; Pielak, G. J. *J. Am. Chem. Soc.* **1995**, *117*, 1675. (c) Caffrey, M. S.; Cusanovich, M. S. *Biochim. Biophys. Acta* **1994**, *1187*, 277.
(67) (a) Gooley, P. R.; MacKenzie, N. E. *FEBS Lett.* **1990**, *260*, 225. (b) Gooley, P. R.; Caffrey, M. S.; Cusanovich, M. A.; MacKenzie, N. E. *Biochemistry* **1992**, *31*, 433.
(68) Berry, M. J.; George, S. J.; Thomson, A. J.; Santos, H.; Turner, D. L. *Biochem. J.* **1990**, *270*, 413.
(69) Costa, H. S.; Santos, H.; Turner, D. L.; Xavier, A. V. *Eur. J. Biochem.* **1992**, *208*, 427.

protein should allow protonation of a former histidine ligand in the reduced form of this protein, but not in ferrocytochrome b_5, has yet to be determined, but the observation points out the very major role of the protein in modulating complex stabilities and reduction potentials.

Conclusions and Summary. The equilibrium constants for six iron porphyrinates with four pyridines and two imidazoles have been determined. The size of the equilibrium constants generally increases as the size of the phenyl 2,6 substituents increases, and to a lesser degree with "electron-withdrawing" substituents producing larger constants. The trend in the size of equilibrium constants differs from the trend in reduction potentials observed, especially for the free iron tetraphenylporphyrinates, and to some extent the complexed iron tetraphenylporphyrinates, where the observed values of $E_{1/2}$ directly follow the traditionally-expected electronic effects of the phenyl 2,6 substituents. For iron(III), $\log \beta_2^{III}$ is linearly related to the pK_a of the conjugate acid of the coordinating pyridine, while the iron(II) constants for the hindered iron(II) tetraphenylporphyrinates have little or no dependence on the base strength the various pyridines, but are leveled to a particular value for each porphyrinate. The linear free energy dependence of the iron(III) complexes is believed to be due to a combination of electronic and steric effects and is magnified by the charge on the iron center. Contrary to popular belief, 2-methylimidazole can form bis complexes with iron(II) tetraphenylporphyrinates, but only if bulky *ortho* substituents (Cl, Br, CH_3) are present.

The equilibrium constants for iron tetraphenylporphyrinate−axial ligand complexes are several orders of magnitude smaller than those reported in a similar study[33] that was carried out in methylene chloride. While the present study was performed in DMF, where the equilibrium constants measured are actually exchange constants, the results obtained in this study should differ from those of the previous study by a constant amount. This is not the case, and we cannot account for the large discrepancies between our results and those reported earlier.

Finally, this work has shown that the substituted pyridines would serve as very poor axial ligands for the heme in the cytochromes. The differences in the equilibrium constants between the iron(III) and iron(II) forms are large and could possibly result in loss of the heme upon oxidation or at least loss of one or both axial ligands, which could lead to unfolding of the protein and loss of heme. *N*-Methylimidazole, a closer analog to the amino acid histidine, universally has very small differences in iron(II) and iron(III) equilibrium constants and thus would be a very good ligand for the heme.

Acknowledgment. The support of this work by the National Institutes of Health, Grant DK 31038, is gratefully acknowledged. The authors wish to thank Dr. D. Brooke Hatfield for writing the software for transfer of the electrochemical data from the PAR Headstart program to Quattro.

Supporting Information Available: Figures S1−S4, showing plots of $\log \beta_2^{II}$ and $\log \beta_2^{III}$ vs $pK_a(BH^+)$ for the $((2,6\text{-}Br_2)_4$-, $((2,6\text{-}Cl_2)_4$-, $((2,6\text{-}F_2)_4$-, and $((2,6\text{-}(OMe)_2)_4$(TPP)Fe complexes with the pyridines and imidazoles of this study (4 pages). Ordering information is given on any current masthead page.

IC960491H